

Article

Phosphorous (V) Corrole Fluorophores for Nitrite Assessment in Environmental and Biological Samples

Fabrizio Caroleo ¹, Giovanni Diedenhofen ¹, Alexandro Catini ² , Corrado Di Natale ² , Roberto Paolesse ¹ 
and Larisa Lvova ^{1,*} 

¹ Department of Chemical Science and Technologies, University of Rome “Tor Vergata”, 00133 Rome, Italy; crlfrz01@uniroma2.it (F.C.); giovini.diden@gmail.com (G.D.); roberto.paolesse@uniroma2.it (R.P.)

² Department of Electronics Engineering, University of Rome “Tor Vergata”, 00133 Rome, Italy; catini@ing.uniroma2.it (A.C.); dinatale@uniroma2.it (C.D.N.)

* Correspondence: larisa.lvova@uniroma2.it; Tel.: +39-06725974732

Abstract: Two phosphorous (V) corrole complexes, [5,10,15-pentafluorophenyl corrole] phosphorous (V) (**PFCorr**) and [10-(4-trimethylsilylphenyl)-5,15-dimesityl-corrole] phosphorous (V) (**PCorr**) were synthesized and tested as nitrite-sensitive fluorophores. Fluorimetry studies on ligand sensitivity towards anions were carried out in solution, then inside polymeric membrane optodes deposited on glass, and finally by functionalized SiO₂ nanoparticles deposited on a paper support. The selective fluorescence quenching was registered upon addition of an increasing amount of NO₂[−] ions for both ligands. The influence on the **PFCorr** optode’s response of the lipophilic sites’ functionalization was investigated. The sensors’ suitability for nitrite assessment in natural waters at levels 10-fold lower than the WHO’s recommended maximum concentration level of 3 mg/L was demonstrated.

Keywords: phosphorous corrole fluorophores; nitrite detection; optical chemical sensor; silica nanoparticles



Citation: Caroleo, F.; Diedenhofen, G.; Catini, A.; Di Natale, C.; Paolesse, R.; Lvova, L. Phosphorous (V) Corrole Fluorophores for Nitrite Assessment in Environmental and Biological Samples. *Chemosensors* **2022**, *10*, 107. <https://doi.org/10.3390/chemosensors10030107>

Academic Editor: Eugenia Fagadar-Cosma

Received: 1 February 2022

Accepted: 7 March 2022

Published: 10 March 2022

Publisher’s Note: MDPI stays neutral with regard to jurisdictional claims in published maps and institutional affiliations.



Copyright: © 2022 by the authors. Licensee MDPI, Basel, Switzerland. This article is an open access article distributed under the terms and conditions of the Creative Commons Attribution (CC BY) license (<https://creativecommons.org/licenses/by/4.0/>).

1. Introduction

Nitrites have important effects on human health and the environment, and their quantitative assessment has been an important and challenging analytical task over the last two decades [1,2]. Nitrite ion (NO₂[−]) monitoring is especially important for potable water and foodstuff quality control, in wastewater treatment, in agriculture, and in fish farming. In particular, the recommended values for freshwater fish species are quite restrictive, requiring nitrite ions concentrations lower than 0.1 mg/L [2].

Usually, nitrites are not present in the environment in significant concentrations (except in reducing media), as nitrate is the more stable oxidation state. Particular conditions are required for nitrites’ formation in the natural environment, such as microbial reduction in ingested nitrate in vivo; for instance, the bacteria *Nitrosomonas europaea* were found to be involved in nitrite production from ammonia [3] during stagnation of nitrate-containing and oxygen-poor drinking-water inside steel pipes. In order to gain a complete estimation of the total inorganic forms of nitrogen present in analyzed media, nitrite screening is always made in parallel to nitrates. The nitrate ion (NO₃[−]) is found naturally in the environment and it is present at varying concentrations in all plants. Nitrates can reach both surface water and groundwater because of agricultural activity, from wastewater disposal and from the oxidation of nitrogenous waste products in human and animal excreta, including septic tanks. Surface water nitrate concentrations can change rapidly owing to surface runoff of fertilizer, uptake by phytoplankton, and denitrification by bacteria, but groundwater concentrations generally show relatively slow changes [2]. The most common human exposure to nitrite- and nitrate ions is through vegetables and diet proteins (nitrite is used as a preservative in many cured meats). In some circumstances, however, drinking-water can make a significant contribution to nitrate- and, occasionally, nitrite intake. In the

case of bottle-fed infants, drinking-water can be the major external source of exposure to both NO_3^- and NO_2^- ions. By its turn, nitrite can bind to hemoglobin, the oxygen transporter molecule in the red blood cells; this interaction produces methemoglobin that binds oxygen tightly. When the methemoglobin concentration in blood is $\geq 10\%$, clinically relevant cyanosis known as ‘blue-baby syndrome’, can appear and be fatal for a child. This negative effect of nitrite on humans was first investigated by Comly in 1945 [4]. Studies have also shown a correlation between nitrate and nitrite ingestion and increase in gastric cancer formation risks; in 2010 the IARC (International Agency for Research on Cancer) has classified “nitrate or nitrite (ingested) under conditions that result in endogenous nitroization” as probably carcinogenic to humans [5]. In fact, in the body NO_2^- ions form carcinogenic nitrosamines [1] when they bind with secondary amines, and it is hence essential to monitor the nitrite levels in the environment and especially in samples causing health concerns.

Traditionally nitrites are determined in solution by spectrophotometry in the presence of specific ligands [6] or by electrochemical techniques employing bio- and chemical sensors, such as ISEs [7–11]. Optical chemical sensors have been employed to a much smaller degree, despite their evident benefits, such as simplicity in preparation, no necessity of a sophisticated and high energy-consuming hardware, and no wire connections with detectors. Moreover, the analytically useful optical sensor output can be registered with common electronic devices, such as smartphones, or even without any power supply in a ‘naked-eye’ mode, when the sensor luminescence intensity change upon interaction with the analyte may be registered visually (especially useful in situations of rapid qualitative analysis and alarm cases). There is, hence, an unmet need to develop easy-to-handle and inexpensive optical sensors for fast and effective nitrite assessment. However, analyses of the last 5 years of publications on NO_2^- -sensor development have shown that less than 10% of all research is dedicated to sensors with optical transduction; this research is mainly dedicated to nanomaterial-based sensors, such as metal and metal-oxide nanoparticles [12,13], quantum dots [14], or liquid crystals [15]. Some applications of polymeric sensing materials doped with nitrite-selective ligands for optode development are also reported [16]. The accurate selection of the appropriate macromolecular ligands selectively binding to the target analyte has permitted the development of selective optodes for several inorganic anions, including nitrites [17–20]. Among these ligands (or ionophores) metalloporphyrin and metallocorrole complexes are particularly suitable for anion sensing through metal–anion coordination, a type of Lewis acid–base interaction [21,22]. The metallocorroles have significant potential to be integrated in optical sensors, a sensor type that has seen many technological developments and applications, including in a wide variety of smartphones [23,24]. This combination, when applied to environmental nitrate monitoring, could result in sensors that are less expensive, more portable, with greater ease of use and more disposable reagents.

The present work investigates the properties of corrole ligands, 5,10,15-pentafluorophenyl corrole of phosphorous (V) (**PFCorr**), and [10-(4-trimethylsilylphenyl)-5,15-dimesityl-corrole] phosphorous (V) (**PCorr**) previously tested in [25], for the development of selective optical sensors for rapid and low-cost detection of nitrites in natural samples with a particular attention to water quality monitoring, Figure 1. Preliminary fluorimetric studies on ligands’ sensitivity towards different anions carried out in solution and inside the solvent polymeric membranes [26] have been advanced in the present work. Moreover, we investigated the properties of silica nanoparticles with anchored **PFCorr** units uploaded on a paper support for selective nitrite sensing. In each of these conditions the selective ligand’s fluorescence quenching was registered upon addition of an increasing amount of NO_2^- ions. The sensing properties of **PFCorr** on different supports were investigated in order to detect the effectiveness of nitrite assessment at recommended concentrations levels.

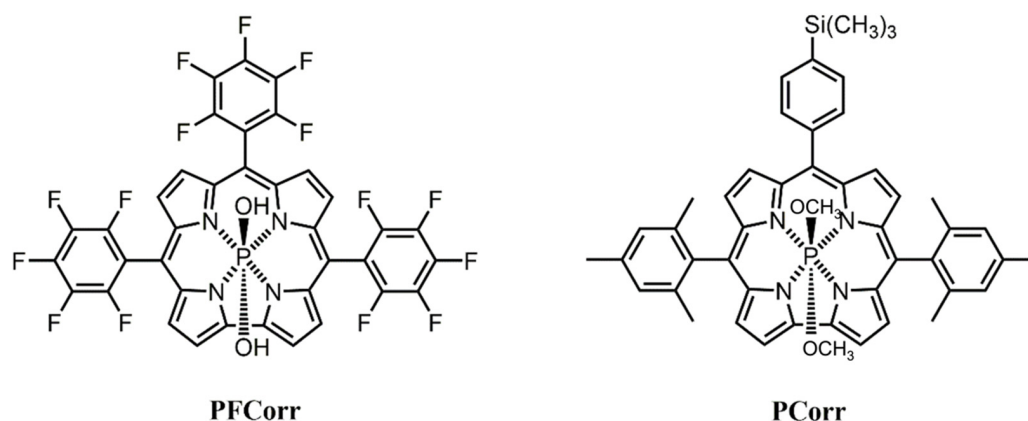


Figure 1. Chemical structures of studied phosphorous (V) corroles fluorophores.

2. Materials and Methods

The **PCorr** and **PFCorr** were synthesized and fully characterized by NMR, UV-Visible and photoluminescence spectroscopy in our laboratories. For synthesis of [10-(4-trimethylsilylphenyl)-5,15-dimesityl-corrole] phosphorous (V) (**PCorr**) the procedure reported in [27] was adopted. The 5,10,15-pentafluorophenyl corrole of phosphorous (V), **PFCorr** complex was obtained by a two-step procedure including free base corrole synthesis and its subsequent metalation. The procedure is schematically represented in Figure 2.

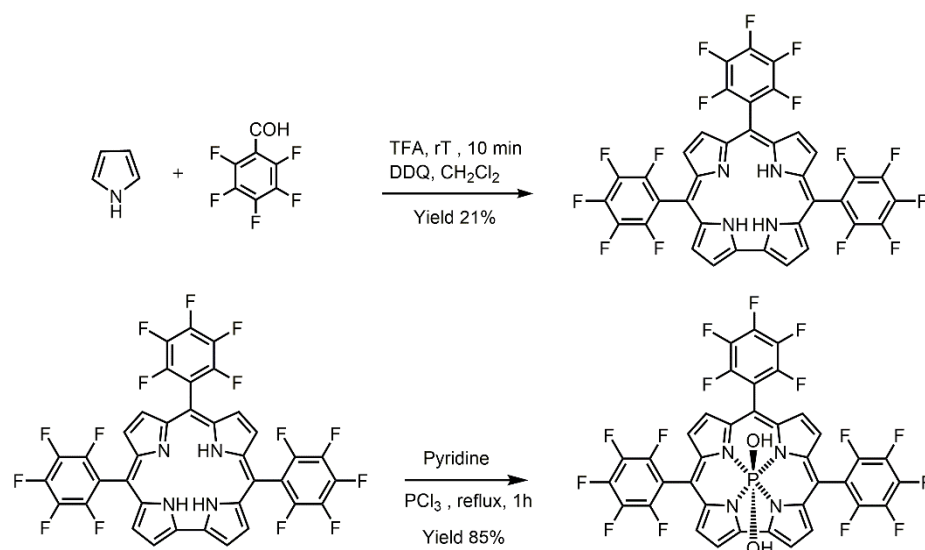


Figure 2. The schematic representation of two-step **PFCorr** synthesis.

The Poly(vinyl chloride) (PVC) high molecular weight, tris(2-ethylhexyl) phosphate (TOP), tetradecylmethyammonium chloride (TDACl), tetrabutylammonium nitrite (TBANO₂), tetrahydrofuran (THF), chloroform (CHCl₃), 2-(N-morpholino) ethanesulfonic acid (MES), NaNO₂, NaCl, NaBr, NaNO₃, CH₃CO₂Na, NaClO₄, NaSCN, NaHCO₃, and Na₂SO₄ salts were from Sigma-Aldrich (Milan, Italy). Ultrapure water was used for aqueous solution preparation. THF was freshly distilled prior to use. All the other chemicals were of analytical grade and used without further purification.

Polymeric membranes were prepared by incorporation of 1 wt% of **PFCorr** and 0.5–5 wt% of TpCIPBK inside a polymeric matrix containing PVC and plasticizer in 1:2 ratio by weight. Membranes with a total weight of about 100 mg, were dissolved in 1 mL of THF. Ten microliters of each membrane cocktail was cast onto transparent glass slides, the THF solvent was allowed to evaporate overnight, and afterwards the ‘disposable’ optode sensors were tested in individual solutions of several anions on 0.01 M MES pH 5.5 background in

a 1.0×10^{-8} – 1.0×10^{-2} M concentration range. The calibration solutions were obtained by consecutive additions of calculated amounts of corresponding 1 M stock solution of different salts.

SHIMAZU RF-1501 fluorimeter (Shimadzu Europe, Duisburg, Germany) was employed for tests in solutions. An amount of 2.5 mL of 6×10^{-8} M **PFCorr** solution was titrated with 10^{-2} M, 10^{-4} M and 10^{-5} M stock solutions of tetrabutylammonium nitrite (TBANO₂) in chloroform directly in a quartz cuvette of 1 cm, and light was passed upon the excitation at 413 nm (wavelength of **PFCorr** Soret band in the absorption spectra). The fluorescence spectra were registered 10 min after each nitrite concentration addition. In total, eight additions of TBANO₂ were performed to reach a cumulative amount of 125 µL added to the cuvette. For the fluorimetric selectivity tests, 1 M aqueous stock solutions of the sodium salts of the following anions were used: NO₂[−], NO₃[−], SCN[−], ClO₄[−], Cl[−], and Br[−]. A single calculated addition of 1 M stock solution was made in order to obtain a final 6×10^{-2} M concentration of each interfering ion to the 6×10^{-8} M **PFCorr** solution in DMSO. The fluorescence spectra were recorded 10 min after the addition of an interfering ion in order to exclude the dilution effect for the emission quenching. For the testing of optodes with PVC-based solvent polymeric membranes doped with **PFCorr** and **PCorr**, a UV-lamp (365 nm) or commercial blue-colored Light Emitting Diode (LED, 380 nm) served as a monochromic excitation light source. For experiments with the UV-lamp, 5 µL of solutions containing different (increasing) concentrations of the analyzed anion were deposited on sensing spots obtained by drop-casting **PFCorr**- and **PCorr**-doped PVC-based membranes on a glass support. The optode emission signal, upon illumination at 365 nm, was registered 3 min after analyte addition from the fixed distance of 10 cm by means of a common smartphone camera, and the luminescence variations were then extracted from images and transformed into analytically useful digital signals using Matlab software (v.7.9, 2009, The MathWorks, Inc., Natick, MA, USA). Due to the enhanced photosensitivity of the membranes, and in order to avoid photo degradation problems, all the experiments were carried with ‘disposable’ optical sensors, deposited on a transducer a few times prior to the testing. **PFCorr**- and **PCorr**-doped PVC membranes were stored in the dark before use. The measurements were repeated in triplicate. The Photoassisted Technique (PT) set up was used for measurements with a blue-colored InGaN LED (Roithner LaserTechnik, Wien, Austria, model H2A1-H385), as a monochromic external light source; and a frontally placed digital webcam (Philips S.p.A, Milan, Italy, model Philips SPC900NC) for notebook (resolution of 352×288 pixels) was used as a signal detector, as described in detail in our previous work [25]. Glass slides (0.7 cm \times 3.0 cm size) with sensing membranes deposited on them were vertically immersed in polystyrene cuvettes of 1 cm path length and then laterally illuminated with an LED, and the responses of the sensing membranes were recorded from three channels representing the main visible spectrum colors: red, R (630 nm), green, G (530 nm), and blue, B (480 nm). The measurement cell was shielded from external illumination. The luminescence intensity was calculated as:

$$I = (R + G + B)/(3 \times 255)$$

where R, G, and B correspond to the sensing membranes luminescence intensities at RGB channels, and normalized to the maximum intensity value (255) of the optical signal measured with a webcam detector. The relative optical intensity quenching was estimated as a percentage of I in the absence and in the presence of an analyte, evaluated after a background luminosity subtraction. The duration of the overall sample illumination was 50 s for the LED (during this period 10 photographic shoots were taken every 5 s, and the final optical signal was a mean value of the records) and 10 s for the UV-vis lamp.

The SiO₂ nanoparticles (SO₂NPs) were prepared according to the Stöber method [28], through the hydrolysis and condensation of tetraethyl orthosilicate TEOS in ethanol, in the presence of ammonia as a catalyst. Briefly, to obtain a solution [NH₃] = 0.3 M and [H₂O] = 1 M, 2.4 mL of 28% ammonium hydroxide solution and 2.16 mL of H₂O were added to 120 mL of ethanol and stirred for 10 min to ensure complete mixing. Then 7.5 mL

of TEOS was added ($[\text{TEOS}] = 0.28 \text{ M}$) and the reaction proceeded at room temperature for 24 h. Thereafter the colloidal solution was separated by high-speed centrifuge, and the silica nanoparticles were washed three times with ethanol to remove undesirable particles. The particles were dried in an oven at 100°C for 2 h to prevent further reaction.

The SiO_2 NPs were functionalized with **PFCorr** ($\text{SiO}_2\text{NPs@PFCorr}$) through a two-step method called ‘post nanoparticles coating’, in which the **PFCorr** was added to a suspension of SiO_2 nanoparticles already synthesized. After a 2 h thermal treatment at 150°C to remove physisorbed water, SiO_2 nanoparticles (80 mg) prepared previously in the first step were put in a glass flask equipped with 8 mL of toluene, followed by sonication to ensure dispersion. Five milligrams of **PFCorr** were then added to the flask and the mixture was stirred and refluxed at 110°C for 3 h. The solid was recovered by ultracentrifugation and repeatedly washed with CH_2Cl_2 , acetone, ethanol, and toluene in order to remove any excess of non-linked corrole. Particles were finally dried at 150° for 2 h. For the titration of $\text{SiO}_2\text{NPs@PFCorr}$ with NO_2^- ions, 4 mg of NPs were suspended in 100 mL of THF upon sonication. To this suspension the calculated amount of 1 M TBANO_2 in CHCl_3 was added in order to obtain the required concentration of nitrite ions. The fluorescence emission spectra were measured upon the excitation at 413 nm, 10 min after each addition, maintaining the same instrument setup.

The deposition of the functionalized nanoparticles on a paper support was made by a drop-casting method. The suspension was prepared by sonicating 2 mg of $\text{SiO}_2\text{NPs@PFCorr}$ in 1.5 mL of organic solvent (THF or toluene). Each spot on the filter paper strips Whatman™ (Cat No 1001-150) was made by a micropipette, dripping 150 μL of the previously prepared suspension. The solvent was allowed to dry at room temperature and the operation was repeated 3 times for each spot. The fluorescence quenching of $\text{SiO}_2\text{NPs@PFCorr}$ deposited on the paper support in the presence of increasing concentrations of nitrite ions was registered upon illumination with UV-vis lamp (Vilber Lourmat Sté, Collegein, France, model VL-6.LC) at 365 nm according to the same procedure above-described for PVC-based polymeric membranes.

NMR experiments were performed in CDCl_3 at 25°C and recorded with a Bruker AV400 spectrometer (Bruker, Macerata, Italy) operating at 121.48 MHz (^{31}P). Chemical shifts are given in ppm relative to a CDCl_3 solution of PPh_3 (-6.1 ppm) as an external standard for ^{31}P spectra. For ^{31}P NMR spectroscopy, **PFCorr** was dissolved in a small volume (0.8 mL) of deuterated chloroform, CDCl_3 . Then 200 μL of 1 M TBANO_2 solution in CDCl_3 was added to the **PFCorr** solution in order to reach an excess of nitrites in the solution ($[\text{NO}_2^-] = 0.2 \text{ M}$) to estimate the axial coordination of these anionic species on the central phosphorus atom.

The SEM images were obtained with an LEO 1430 unit (Carl Zeiss Microscopy, LLC, White Plains, NY, USA) using an accelerating voltage of 10 and 15 kV. The SEM samples were prepared by depositing a suspension of $\text{SiO}_2\text{NPs@PFCorr}$ in THF, then the substrate was dried and preserved in an inert atmosphere.

3. Results and Discussion

The sensitivity of [10-(4-trimethylsilylphenyl)-5,15-dimesitylcorrole] phosphorous (V), **PCorr**, to changes in nitrite ions' concentration and ligand luminescence quenching upon analyte concentration growth was demonstrated in our previous work [25]. In this previous research, it was supposed that the quenching fluorescence is caused by an axial coordination of rich electronic density species, such as anions, to the inner P (V) center of the macrocycle. Such coordination was previously reported in literature also for other metallocorroles [20]; the phenomenon generally promotes quenching of corrole fluorescence and the value of this quenching is related to the concentration of anions present in the environment. In order to enhance anion-binding properties and increase ligand fluorescent properties, we introduced a high number of electronegative fluorine side-substituents in the chemical structure of the **PFCorr** ligand (Figure 1). This structural modification is expected to generate a shift of electron density around the peripheral area of the macrocycle leading

to the promoted anionic sensitivity. The luminescence quantum yields, Φ_F , were estimated for both fluorophores in CHCl_3 according to the common procedure [22], and were 0.22 and 0.26 for **PCorr** and **PFCorr**, respectively.

PFCorr showed a great fluorescence emission property in the region 550–680 nm upon the excitation at 413 nm, corresponding to the ligand Soret band absorbance maximum. The external core fluorination procedure, as expected, resulted in enhanced fluorescence quenching in the presence of nitrite ions: significant emission quenching of **PFCorr** at 580 nm was registered in the concentration range from 6×10^{-8} to 6×10^{-2} M (Figure 3a). The selectivity test showed no influence of NO_3^- , Cl^- , Br^- , SCN^- , and ClO_4^- interfering anions present in the same concentration (6×10^{-2} M) in tested solutions on the selective interaction of **PFCorr** ligand with nitrites (Figure 3b).

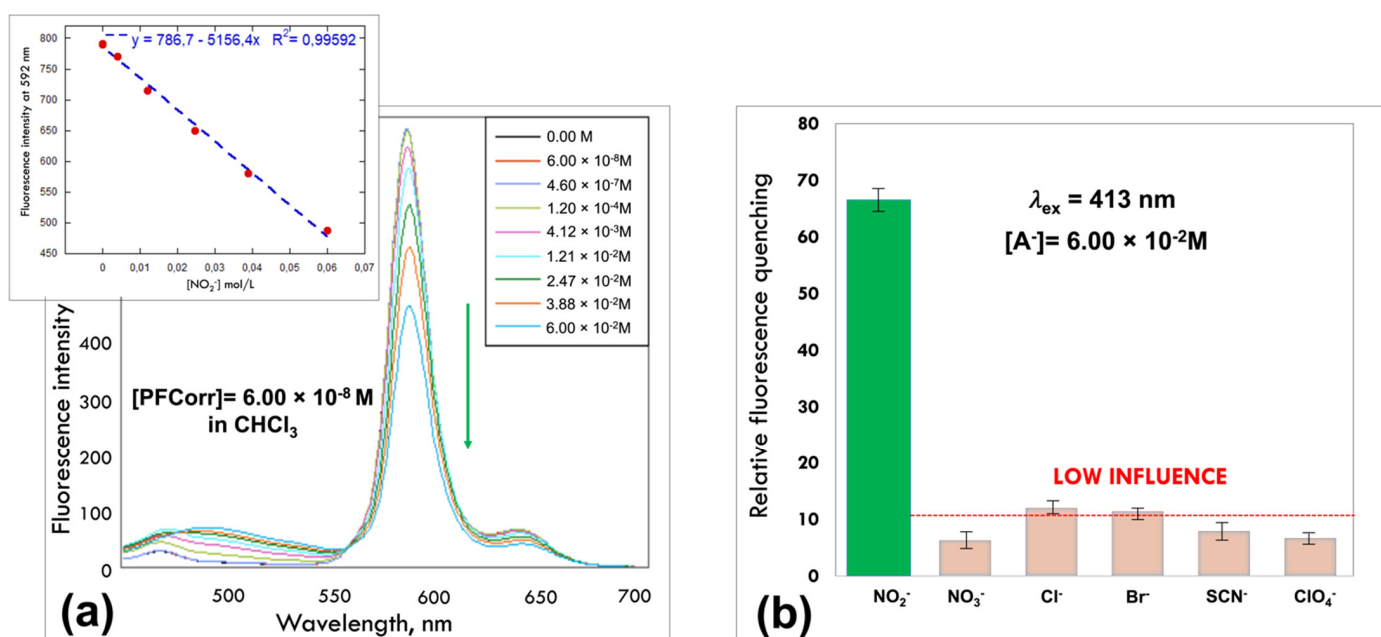


Figure 3. (a) The fluorescence response of 6×10^{-8} M **PFCorr** in CHCl_3 upon addition of increasing concentrations of NO_2^- ions. In the insert: linear regression curve of **PFCorr** fluorescence intensity quenching at 592 nm vs. $[\text{NO}_2^-]$, mol/L; (b) The tests on relative fluorescence quenching of **PFCorr** fluorescence at 580 nm in the individual anion solutions in concentration 6×10^{-2} M; $\lambda_{\text{ex}} = 413$ nm.

The obtained results indicate the high sensitivity of the **PFCorr** ligand to nitrite ions. The coordination of NO_2^- ions as an axial ligand on the central phosphorus was investigated with ^{31}P NMR spectroscopy performed before and after the addition of NO_2^- ions. As shown in Figure 4, the chemical shift for the central phosphorus in pure **PFCorr** was -191.18 ppm, which corresponds to a hexa-coordinated species with two hydroxyl groups as axial ligands [29–31]; upon the addition of the high excess of nitrite anions, $[\text{NO}_2^-] = 0.2$ M, the chemical shift of the phosphorus changes from -191.18 to -190.97 due to the axial coordination of the nitrite ion on the central phosphorus atom of the **PFCorr** ligand.

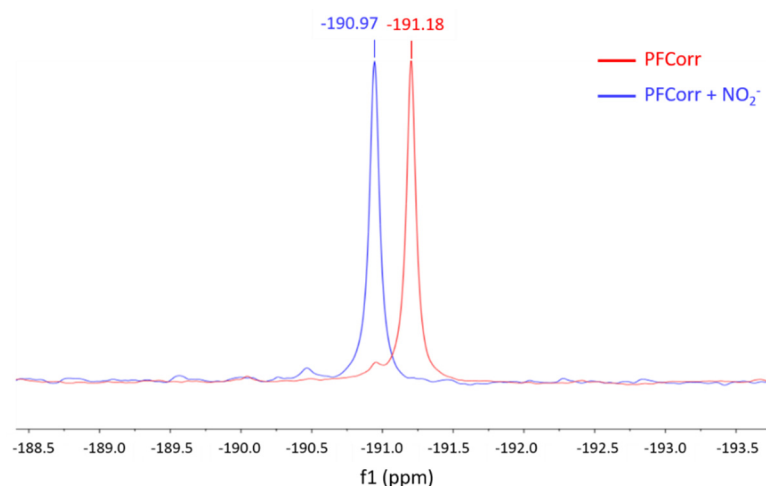


Figure 4. The ^{31}P NMR spectra in CDCl_3 of **PFCorr** before (red) and after (blue) the addition of NO_2^- ions.

The developments of all-solid-state optical sensors are guided by the requirements of practical utility and easy application of these devices. Consequently, the necessity of fast and accurate readouts from optical sensor outputs determines to a high degree the construction of such systems and defines the choice of the appropriate solid support used for ligand immobilization. The immobilization of binding ligands inside a polymeric matrix is one of the most widely applied methods for the bulk ion-selective optodes' development. Moreover, over the past decade, nanomaterials [12–15] and paper-based sensors [23,24,32,33] have been developed for a wide range of analytes, including inorganic anions.

In the next step, with the aim to develop all-solid-state nitrite-selective optodes, we compared the performance of PVC/TOP membranes based on **PFCorr** and previously tested in [25] **PCorr** fluorophores. While in our preliminary study the PVC-based membranes doped with **PCorr** and **PFCorr** were tested as cross-sensitive components in an optical sensor array [26], the results of selectivity tests in solutions confirmed with ^{31}P NMR nitrite-titration of **PFCorr** have given evidence that suggests the possibility of employing this ligand as a fluorophore for the development of an all-solid-state nitrite-selective optode.

The extraction of the target anion inside the polymeric membrane doped with **PFCorr** results in the axial coordination of the corrole–metal complex and yields a fluorescence signal. Depending on the charge of the fluorophore, an addition of different amounts of cationic lipophilic sites, TDA⁺ inside the membrane is required to facilitate the anion extraction. The compositions of the studied membranes are listed in Table 1.

Table 1. Compositions of tested **PFCorr**- and **PCorr**-doped membranes, PVC:TOP = 1:2 ratio by weight.

Membrane	Ligand, wt%	TDACl, wt%	L:TDACl, Molar Ratio
Mb 1.1	PFCorr , 0.5	0.5	1:1:1
Mb 1.2	PFCorr , 0.5	1	1:1.8
Mb 1.3	PFCorr , 1.0	5	1:4.6
Mb 2.1	PCorr , 0.5	0.5	1:1.1
Mb 2.2	PCorr , 1.0	5	1:4.9

The amount of fluorophores in a membrane series was 0.5 and 1 wt%, while 0.5, 1, and 5 wt% of TDACl anion-exchanger were added. These amounts correspond to the 1:1, 1:2, and 1:5 molar ratios between ligand and anion-exchanger amounts for **PFCorr** based membranes Mb1.1–Mb.1.3, respectively, and to 1:1 and 1:2 molar ratio between ligand and anion-exchanger amounts for **PCorr**-based membranes Mb2.1–Mb.2.2, respectively

(Table 1). The fluorimetric response toward NO_2^- ions was investigated for membrane spots drop-cast on glass slides in a 0.01 M MES background solution with pH 5.5 in the concentration range 1.0×10^{-6} – 1.0×10^{-1} M.

The fluorimetric response with the widest linear range was recorded for the optode with Mb 1.3, doped with 1 wt% of **PFCorr** ligand and containing five-fold molar excess of anion-exchanger, TDACl (5 wt%), indicating the prevalent influence of the target anion's transport inside the membrane phase on the optode's sensing properties' improvement (Figure 5).

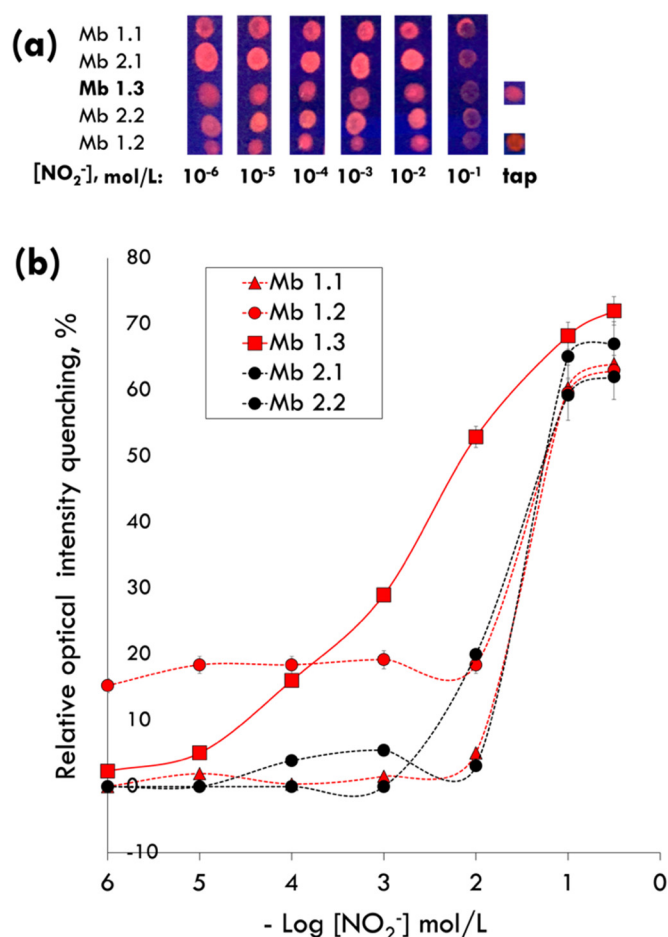


Figure 5. (a) The photograph of **PFCorr**- and **PCorr**-based optodes in solutions of NO_2^- ions on 0.01 M MES pH 5.5 background upon excitation at 365 nm with UV-lamp; (b) the relative optical intensity quenching (on red channel of RGB color scale, %)-based calibration curves toward NO_2^- ions.

As it can be seen from the Figure 5, the visibly observed luminescence intensity quenching of the sensing material indicates the suitability of the **PFCorr**-based optodes to perform fast monitoring of nitrite ions in concentrations up to 10^{-1} M with a low detection limit estimated as 0.27 mg/L, which is one order of magnitude lower than the maximum recommended NO_2^- concentration level of 3 mg/L in drinking water [34]. No significant luminescence quenching of membranes Mb3.1 and Mb2.1 doped respectively with **PFCorr** and **PCorr** was registered in tap water samples (laboratory tap water from the 'Tor Vergata' zone of the city of Rome, Italy, with a medium nitrite content around 0.1 mg/L according to the ACEA data [35]) (Figure 5).

Further, in order to improve the performances of **PFCorr**-based nitrite-selective optodes, we exploited the possibility to anchor ligands on the surface of silica nanoparticles, SiO_2NPs , taking advantage of the higher accessibility of sensing sites to the analyte and enhanced emission quenching through the so-called 'dye–dye interactions' between prox-

imal ligands [36]. SiO₂NPs were chosen since they are not toxic, can be obtained with a simple synthetic procedure, and are inexpensive [28]. The PFCorr functionalization of SiO₂NPs was made by the ‘post-coating method’ procedure, that consists of two steps, as described in detail in the Section 2. The anchoring of PFCorr on SiO₂NPs occurs through the axial coordination of hydroxyl groups present on the silica surface to the corrole’s central phosphorus. The wider surface area of SiO₂NPs significantly increases the number of analyte–ligand interactions, allowing the coordination of many sensing corrole units with free axial positions available for analyte binding that leads to a magnification of the sensing response (Figure 6a). Moreover, the phenomena of ligand aggregation typical in solution (or inside a polymeric membrane) is eliminated for SiO₂NPs@PFCorr due to the rigid fluorophore fixation on NPs; the axial nitrite coordination and the prevalence of SiO₂NPs@PFCorr-NO₂⁻ complexes with 1:1 stoichiometry is expected. The PFCorr functionalization of the SiO₂NPs’ surface was confirmed by UV-vis spectra; while by SEM and fluorescent microscopy the morphologies and the responses to the light exposure of hybrid assemblies were studied (Figure 6b–d, respectively).

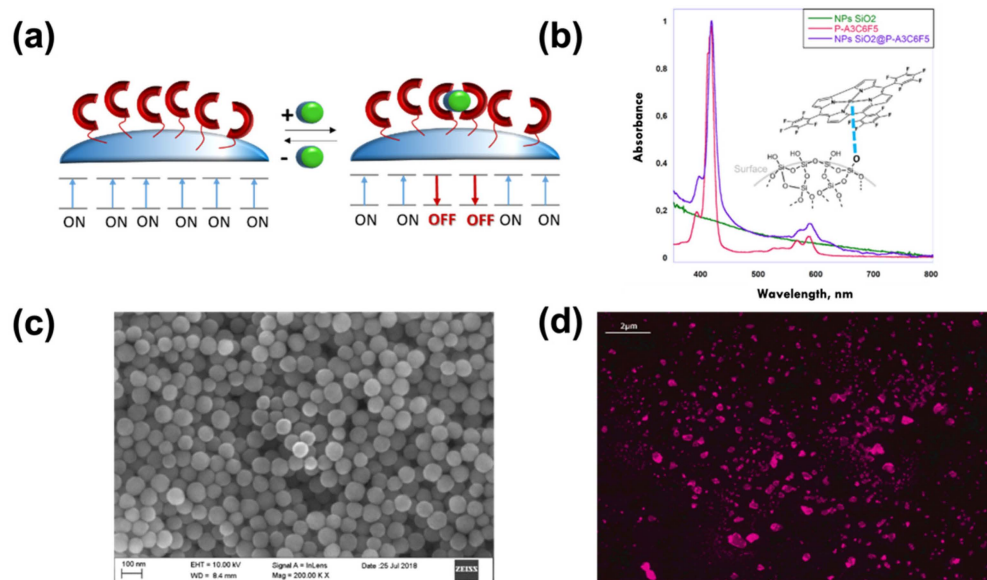


Figure 6. (a) Illustration of NPsSiO₂@corrole dye–dye interaction’s effect on nitrite ion sensitivity; (b) the UV-vis spectrum; (c) SEM; and (d) the optical fluorescent microscopy images of SiO₂NPs@PFCorr hybrid assemblies. For optical fluorescent microscopy SiO₂NPs@PFCorr were dispersed in ethanol.

The SiO₂NPs@PFCorr’s assembling response to nitrite anions was first checked in an aqueous suspension at increasing concentrations of analyte. The tests showed promising results in terms of the quenching effect of corrole fluorescence in the presence of nitrites. As seen in Figure 7, the emission spectra recorded at a determinate nitrite ion concentration, [NO₂⁻] = 4 × 10⁻³ M, showed a much greater fluorescence quenching for hybrid assemblies compared to the response of the phosphorous corrole dissolved in solution without silica nanoparticles as a solid support.

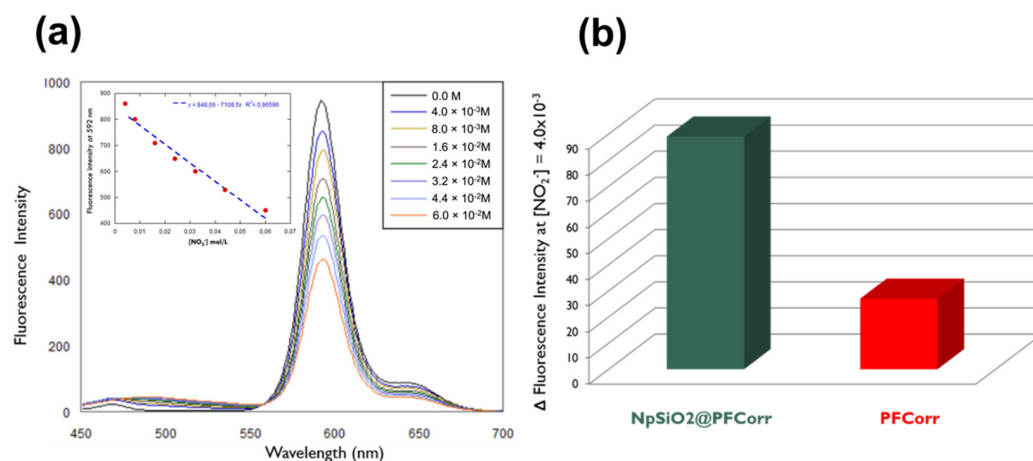


Figure 7. (a) Fluorescence response of $\text{SiO}_2\text{NPs@PFCorr}$ toward increasing concentration of nitrites in aqueous solution. In the insert: linear regression curve of $\text{SiO}_2\text{NPs@PFCorr}$ fluorescence intensity quenching at 592 nm vs. $[\text{NO}_2^-]$, mol/L; (b) comparison of absolute fluorescence intensity quenching value of **PFCorr** ligand solution and $\text{SiO}_2\text{NPs@PFCorr}$ suspension in the presence of nitrite in concentration $[\text{NO}_2^-] = 4 \times 10^{-3}$ M.

Finally, in order to apply $\text{SiO}_2\text{NPs@PFCorr}$ to assemble on a solid support in an optical device for fast and easy in situ measurements, they were deposited on simple filter paper Whatman™ strips. The porosity of the paper allowed a uniform distribution of the nanoparticles on the cellulose fibers inside the material, avoiding leaching of the nanoparticles from the paper support during the liquid samples' analysis. In Figure 8a the SEM image demonstrates the $\text{SiO}_2\text{NPs@PFCorr}$ distribution on the cellulose fibers. Figure 8b shows preliminary tests performed on paper strips using UV-lamp excitation (365 nm) for $\text{SiO}_2\text{NPs@PFCorr}$ deposited from THF and toluene (top) and the response of on-paper $\text{SiO}_2\text{NPs@PFCorr}$ /THF assembly in the aqueous solutions with increasing nitrite concentrations, drop-cast on the surface of the sensing spots (bottom). The obtained results demonstrate the potential of the **PFCorr** ligand for optical nitrate ions, sensing both inside the all-solid state optodes based on polymeric membranes or in on-paper deposited $\text{SiO}_2\text{NPs@PFCorr}$ assemblies. In the latter case the instrument setup should be further optimized, in order to increase the potential of this innovative optical system.

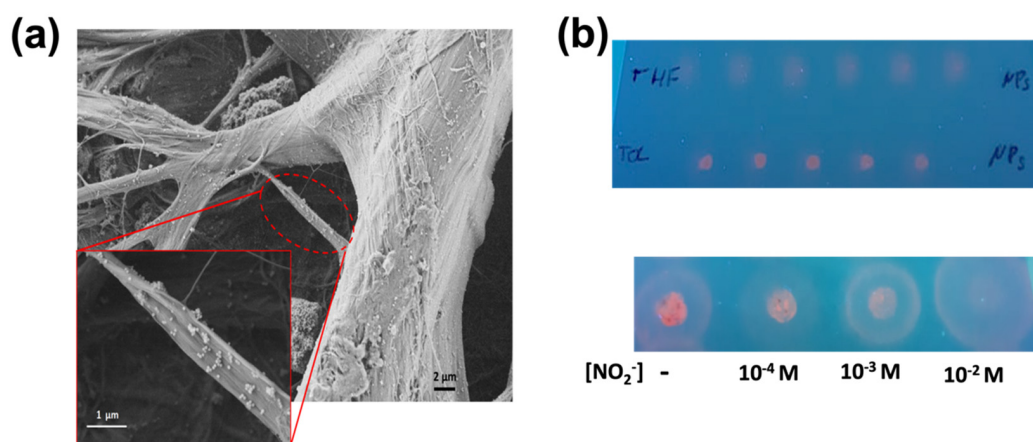


Figure 8. (a) SEM image of $\text{SiO}_2\text{NPs@PFCorr}$ distribution on cellulose fibers; (b) the pictures of $\text{SiO}_2\text{NPs@PFCorr}$ deposited on paper support from THF and toluene (top) and $\text{SiO}_2\text{NPs@PFCorr}$ /THF assemblies response to aqueous solutions of NO_2^- of different concentration upon UV-lamp excitation (365 nm) (bottom).

4. Conclusions

Fluorimetric studies in solution proved that in the presence of nitrites the newly synthesized **PFCorr** ligand gives evidence of selective fluorescence emission quenching. These results make **PFCorr** an ideal candidate as a sensing material for the development of optical sensing devices for nitrite detection. In order to develop an all-solid-state optical sensor and solve the issue of ligand insolubility in water, the **PFCorr** ligand was introduced inside PVC membranes and also was successfully coordinated onto the surface of silica nanoparticles and deposited on paper strips for a possible application in situ, maintaining the guiding concept of developing a fast and low-cost device. This demonstrates the suitability of **PFCorr**-based optodes to perform fast monitoring of nitrite ions in concentrations ranging from 10^{-6} to 10^{-1} M with a low detection limit estimated as 0.27 mg/L; lower than the maximum recommended NO_2^- concentration level of 3 mg/L in drinking water. The further optimization of a $\text{SiO}_2\text{NPs@PFCorr}$ assemblies-based system is now in progress in our laboratories in order to explore and extend the potential of this innovative system for the optical sensing of nitrites in environmental and biological samples.

Author Contributions: Conceptualization, L.L. and R.P.; methodology F.C., G.D. and A.C.; investigation, F.C. and G.D.; writing—original draft preparation, L.L., F.C. and R.P.; writing—review and editing, F.C., R.P. and L.L.; supervision, R.P.; project administration, L.L.; funding acquisition, R.P., A.C. and C.D.N. All authors have read and agreed to the published version of the manuscript.

Funding: Larisa Lvova gratefully acknowledges the financial support from the Department of Chemical Sciences and technologies of “Tor Vergata” University (project ORIENTATE 2021).

Institutional Review Board Statement: Not applicable.

Informed Consent Statement: Not applicable.

Data Availability Statement: Not applicable.

Conflicts of Interest: The authors declare no conflict of interest.

References

1. Lijinsky, S.S.W.; Epstein, S.S. Nitrosamines as Environmental Carcinogens. *Nature* **1970**, *225*, 21. [[CrossRef](#)] [[PubMed](#)]
2. World Health Organization. *Guidelines for Drinking-Water Quality: Fourth Edition Incorporating the First Addendum*; WHO: Geneva, Switzerland, 2017.
3. Chain, P.J. Complete Genome Sequence of the Ammonia-Oxidizing Bacterium and Obligate Chemolithoautotroph *Nitrosomonas europaea*. *J. Bacteriol.* **2003**, *185*, 2759–2773. [[CrossRef](#)] [[PubMed](#)]
4. Comly, H.H. Cyanosis in infants caused by nitrates in well-water. *JAMA* **1945**, *129*, 112–116. [[CrossRef](#)]
5. *Ingested Nitrate and Nitrite, and Cyanobacterial Peptide Toxins—IARC Monographs on the Evaluation of Carcinogenic Risks to Humans*; International Agency for Research on Cancer (IARC)—World Health Organization (WHO): Geneva, Switzerland, 2010; Volume 94.
6. *Standard Methods for the Examination of Water and Waste Water*; American Public Health Association: New York, NY, USA, 1995.
7. Moretto, L.M.; Ugo, P.; Zanata, P.M.; Martin, G.C.R. Nitrate Biosensor Based on the Ultrathin-Film Composite Membrane Concept. *Anal. Chem.* **1998**, *70*, 2163. [[CrossRef](#)]
8. Badea, A.M.; Amine, G.; Palleschi, D.; Moscone, G.; Volpe, A.; Curulli, J. New electrochemical sensors for detection of nitrites and nitrate. *Electroanal. Chem.* **2001**, *509*, 66. [[CrossRef](#)]
9. Shamsipur, M.; Javanbakht, M.; Hassaninejad, A.R.; Sharghi, H.; Ganjali, M.R.; Mousavi, M.F. Highly Selective PVC-Membrane Electrodes Based on Three Derivatives of (Tetraphenylporphyrinato)Cobalt(III) Acetate for Determination of Trace Amounts of Nitrite Ion. *Electroanalysis* **2003**, *15*, 1251–1259. [[CrossRef](#)]
10. Ahmad, F.; Mahmoudi, T.; Ahn, M.S.; Yoo, J.Y.; Hahn, Y.B. Fabrication of sensitive non-enzymatic nitrite sensor using silver-reduced graphene oxide nanocomposite. *J. Colloid Interf. Sci.* **2018**, *516*, 67. [[CrossRef](#)]
11. Yang, S.; Meyerhoff, M.E. Study of Cobalt(III) Corrole as the Neutral Ionophore for Nitrite and Nitrate Detection via Polymeric Membrane Electrodes. *Electroanalysis* **2013**, *25*, 2579–2585. [[CrossRef](#)]
12. Yoon, S.J.; Nam, Y.S.; Lee, J.Y.; Kim, J.Y.; Lee, Y.; Lee, K.B. Highly sensitive colorimetric determination of nitrite based on the selective etching of concave gold nanocubes. *Microchim. Acta* **2021**, *188*, 132. [[CrossRef](#)]
13. Kumar, C.R.R.; Betageri, V.S.; Nagaraju, G.; Suma, B.P.; Kiran, M.S.; Pujar, G.H.; Latha, M.S. Synthesis of Core/Shell (ZnO/Ag) Nanoparticles Using *Calotropis gigantea* and Their Applications in Photocatalytic and Antibacterial Studies. *J. Inorg. Organomet. Polym. Mater.* **2020**, *30*, 3476–3486. [[CrossRef](#)]
14. Yang, X.; Zhang, Y.; Liu, W.; Gao, J.; Zheng, Y. Confined synthesis of phosphorus, nitrogen co-doped carbon dots with green luminescence and anion recognition performance. *Polyhedron* **2019**, *171*, 389–395. [[CrossRef](#)]

15. Ho, T.Y.; Lan, Y.H.; Huang, J.W.; Chang, J.J.; Chen, C.H. Using Diazotization Reaction to Develop Portable Liquid-Crystal- Based Sensors for Nitrite Detection. *ACS Omega* **2020**, *5*, 11809–11816. [[CrossRef](#)] [[PubMed](#)]
16. Yenil, N.; Yemiş, F. Nitrite in Nature: Determination with Polymeric Materials. *Pak. J. Anal. Environ. Chem.* **2018**, *19*, 104–114. [[CrossRef](#)]
17. Mohr, G.J.; Wolfbeis, O.S. Optical nitrite sensor based on a potential-sensitive dye and a nitrite-selective carrier. *Analyst* **1996**, *121*, 1489–1494. [[CrossRef](#)]
18. Badr, I.H.A. Nitrite-selective optical sensors based on organopalladium ionophores. *Anal. Lett.* **2001**, *34*, 2019–2034. [[CrossRef](#)]
19. Wang, L.; Meyerhoff, M.E. Polymethacrylate polymers with appended aluminum(III)-tetraphenylporphyrins: Synthesis, characterization and evaluation as macromolecular ionophores for electrochemical and optical fluoride sensors. *Anal. Chim. Acta* **2008**, *611*, 97–102. [[CrossRef](#)] [[PubMed](#)]
20. Yang, S.; Wo, Y.; Meyerhoff, M.E. Polymeric optical sensors for selective and sensitive nitrite detection using cobalt(III) corrole and rhodium(III) porphyrin as ionophores. *Anal. Chim. Acta* **2014**, *843*, 89–96. [[CrossRef](#)]
21. Lvova, L.; Di Natale, C.; D'Amico, A.; Paolesse, R. Corrole-based ion-selective electrodes. *JPP* **2009**, *13*, 1168–1178. [[CrossRef](#)]
22. Di Natale, C.; Gros, C.P.; Paolesse, R. Corroles at work: A small macrocycle for great applications. *Chem. Soc. Rev.* **2022**, *51*, 1277. [[CrossRef](#)]
23. D'Andrea, A.; Pomarico, G.; Nardis, S.; Paolesse, R.; Di Natale, C.; Lvova, L. Chemical traffic light: A self-calibrating naked-eye sensor for fluoride. *JPP* **2019**, *23*, 117–124. [[CrossRef](#)]
24. Lvova, L.; Pomarico, G.; Mandoj, F.; Caroleo, F.; Di Natale, C.; Kadish, K.M.; Nardis, S. Smartphone coupled with a paper-based optode: Towards a selective cyanide detection. *JPP* **2020**, *24*, 964–972. [[CrossRef](#)]
25. Lvova, L.; Caroleo, F.; Garau, A.; Lippolis, V.; Giorgi, L.; Fusi, V.; Zaccheroni, N.; Lombardo, M.; Prodi, L.; di Natale, C.; et al. A Fluorescent Sensor Array Based on Heteroatomic Macrocyclic Fluorophores for the Detection of Polluting Species in Natural Water Samples. *Front. Chem.* **2018**, *6*, 258. [[CrossRef](#)] [[PubMed](#)]
26. Lvova, L.; Caroleo, F.; Catini, A.; Diedenhoffen, G.; Paolesse, R.; Di Natale, C. Optical sensor array based on P(V) corroles for fluorometric detection of nitrite. In *ISOEN 2019—18th International Symposium on Olfaction and Electronic Nose*; IEEE: Fukuoka, Japan, 2019; p. 8823175. [[CrossRef](#)]
27. Naitana, M.L.; Nardis, S.; Pomarico, G.; Raggio, M.; Caroleo, F.; Cicero, D.O.; Lentini, S.; Prodi, L.; Genovese, D.; Mitta, S.; et al. A Highly Emissive Water-Soluble Phosphorus Corrole. *Chem. Eur. J.* **2017**, *23*, 905–916. [[CrossRef](#)] [[PubMed](#)]
28. Stöber, W.; Fink, A.; Bohn, E.J. Controlled Growth of Monodisperse Silica Spheres in the Micron Size Range. *Colloid Interface Sci.* **1968**, *26*, 62–69. [[CrossRef](#)]
29. Mason, J. *Multinuclear, NMR*; Plenum Press: New York, NY, USA, 1987; p. 369.
30. Ghosh, A.; Ravikanth, M. Synthesis, Structure, Spectroscopic, and Electrochemical Properties of Highly Fluorescent Phosphorus(V)-meso-Triarylcorroles. *Chem. Eur. J.* **2012**, *18*, 6386–6396. [[CrossRef](#)]
31. Ghosh, A.; Lee, W.-Z.; Ravikanth, M. Synthesis, Structure and Properties of a Five-Coordinate Oxophosphorus(V) meso-Triphenylcorrole. *Eur. J. Inorg. Chem.* **2012**, *2012*, 4231–4239. [[CrossRef](#)]
32. Xie, X.; Bakker, E. Ion selective optodes: From the bulk to the nanoscale. *Anal. Bioanal. Chem.* **2015**, *407*, 3899–3910. [[CrossRef](#)]
33. Wang, X.; Zhang, Q.; Nam, C.; Hickner, M.; Mahoney, M.; Meyerhoff, M.E. Ionophore-based anion-selective optode printed on cellulose paper. *Angewan. Chem.* **2017**, *56*, 11826–11830. [[CrossRef](#)]
34. Document WHO/FWC/WSH/16.52. Available online: https://www.who.int/water_sanitation_health/dwq/chemicals/nitrate-nitrite-background-jan17.pdf (accessed on 6 March 2022).
35. Available online: <https://www.gruppo.acea.it/al-servizio-delle-persone/acqua/acea-ato-2/la-qualita-della-tua-acqua> (accessed on 6 March 2022).
36. Reineck, P.; Gómez, D.; Hock Ng, S.; Karg, M.; Bell, T.; Mulvaney, P.; Bach, U. Distance and Wavelength Dependent Quenching of Molecular Fluorescence by Au@SiO₂Core-Shell Nanoparticles. *ACS Nano* **2013**, *7*, 6636–6648. [[CrossRef](#)]